

Selective and sensitive detection of metal ions by plasmonic resonance energy transfer-based nanospectroscopy

Yeonho Choi¹, Younggeun Park², Taewook Kang^{2*} and Luke P. Lee^{1*}

Highly selective and sensitive optical methods for the detection of metal ions have had a substantial impact on molecular biology^{1–3}, environmental monitoring^{4–10} and other areas of research. Here we demonstrate a new method for detecting metal ions that is based on selective plasmonic resonance energy transfer (PRET) between conjugated metal–ligand complexes and a single gold nanoplasmonic probe. In addition to offering high spatial resolution due to the small size of the probe, our method is 100 to 1,000 times more sensitive than organic reporter-based methods^{3–8}. Moreover, it can achieve high selectivity owing to the selective formation of Cu²⁺ complexes and selective resonant quenching of the gold nanoplasmonic probe by the conjugated complexes. We expect that PRET-based metal ion sensing could have applications in cellular imaging, systems biology and environmental monitoring.

Most biological and chemical optical detection methods are primarily based on organic reporters, which are detected by a change in colour⁴ or fluorescence emission spectra^{5–8}. However, chromophores and organic fluorophores have particular limitations with respect to temporal resolution, sensitivity, selectivity or incompatibility with aqueous environments owing to low water solubility. To address these limitations, noble metal nanoparticles (such as gold and silver) have been used as alternative probes. The nanoparticles selectively self-aggregate in the presence of metal ions, and the plasmonic coupling between the particles can be exploited as a method of detection^{9,10}. However, this random plasmonic coupling of self-assembled nanoparticles cannot provide nanoscopic resolution—owing to the aggregation of many particles—or molecular-specific information about the metal ions. These are both very important capabilities that would constitute breakthroughs in metal-ion detection systems.

Here, we present a nanospectroscopic metal-ion detection technology based on metal–ligand coordination chemistry as well as plasmonic resonance energy transfer (PRET). This technique differs fundamentally from previously described detection systems^{3–10} in several aspects. First, this technique provides potentially nanoscopic spatial resolution as well as high sensitivity (due to the large extinction coefficient) by shrinking the dimension of a detection site to a single nanoscale probe. Second, we can achieve molecular specificity through two main mechanisms: the selective formation of a resonant metal–ligand complex on the surface of the gold nanoplasmonic probe, and ion-specific resonant quenching in the Rayleigh scattering. This second phenomenon occurs because of the selective energy transfer (plasmonic quenching) that only takes place if the resonance frequency matching condition between the gold nanoplasmonic probe and the metal–ligand complexes is satisfied.

The underlying concept of our detection system for metal ions is illustrated schematically in Fig. 1. Analogous to the donor–acceptor energy matching in Förster resonance energy transfer (FRET), we found that when the frequency of the electronic absorption band of a molecule is matched with the resonance frequency of the Rayleigh scattering of a plasmonic particle upon conjugation of the particle with the molecules, PRET generates distinguishable spectral resonant quenching on the Rayleigh scattering spectrum¹¹. Owing to their unique electronic transitions (for example, *d–d* transitions), metal–ligand complexes can generate a matched absorption band with Rayleigh scattering frequency, meaning that those metal–ligand complexes are able to be acceptors in PRET (Fig. 1a). Therefore, we would expect that a gold nanoplasmonic particle conjugated with specific ligands could act as a selective probe for a target metal ion with high sensitivity and selectivity by providing the quantitative spectroscopic quenching information as a function of the local concentration of the target near the single probe. This has not been explored yet by most modern optical organic and inorganic probes (Fig. 1a,b).

As a demonstration, our detection system was applied to detect Cu²⁺ in an aqueous solution. Cu²⁺ was chosen as our model system for several reasons: (i) analytical significance in biological and environmental processes^{12–15}; (ii) comparison of the sensing performance: a large number of Cu²⁺ ion detection methods have been reported^{8,16–18}; and (iii) absorption frequency matching (Fig. 1b): the amine complex of Cu²⁺ has optical absorption peaks in the visible range (around 550 nm) coinciding with the scattering peak of our probe. In our experiment, the Cu²⁺ complex, created by two equivalent ethylenediamine ligands (note that the log K_1 (association constant) for the ethylenediamine and Cu²⁺ in solution is 10.75, and log K_2 is 9.28; ref. 19), exhibited a broad absorption band in the visible region centred at 547 nm with full width at half maximum (FWHM) of >90 nm, and gave a deeply blue–purple solution (see Supplementary Fig. S1).

Our nanoplasmonic probe is 50 nm in diameter to ensure a sufficient intensity of light scattering, and is composed of gold, which allows for the binding of the ethylenediamine moiety on the surface and can therefore selectively recognize Cu²⁺ in the aqueous solution. The preparation of the probe consists of the following steps (see Supplementary Fig. S2 for more details): (i) immobilization of gold particles on a glass slide; (ii) self-assembly of 3-mercaptoptrimethoxysilane (MPTMS) on the surface of the particles; and (iii) hydrolysis of the methoxy groups²⁰ of MPTMS and silanization of *N*-[3-(trimethoxysilyl)propyl]ethylenediamine (TMSen). The scattering images and spectra of individual functionalized gold nanoplasmonic

¹Biomolecular Nanotechnology Center, Berkeley Sensor and Actuator Center, Department of Bioengineering, University of California at Berkeley, Berkeley, California 94720, USA, ²Department of Chemical and Biomolecular Engineering, Sogang University, Seoul, 121-742, Korea. *e-mail: twkang@sogang.ac.kr; lplee@berkeley.edu

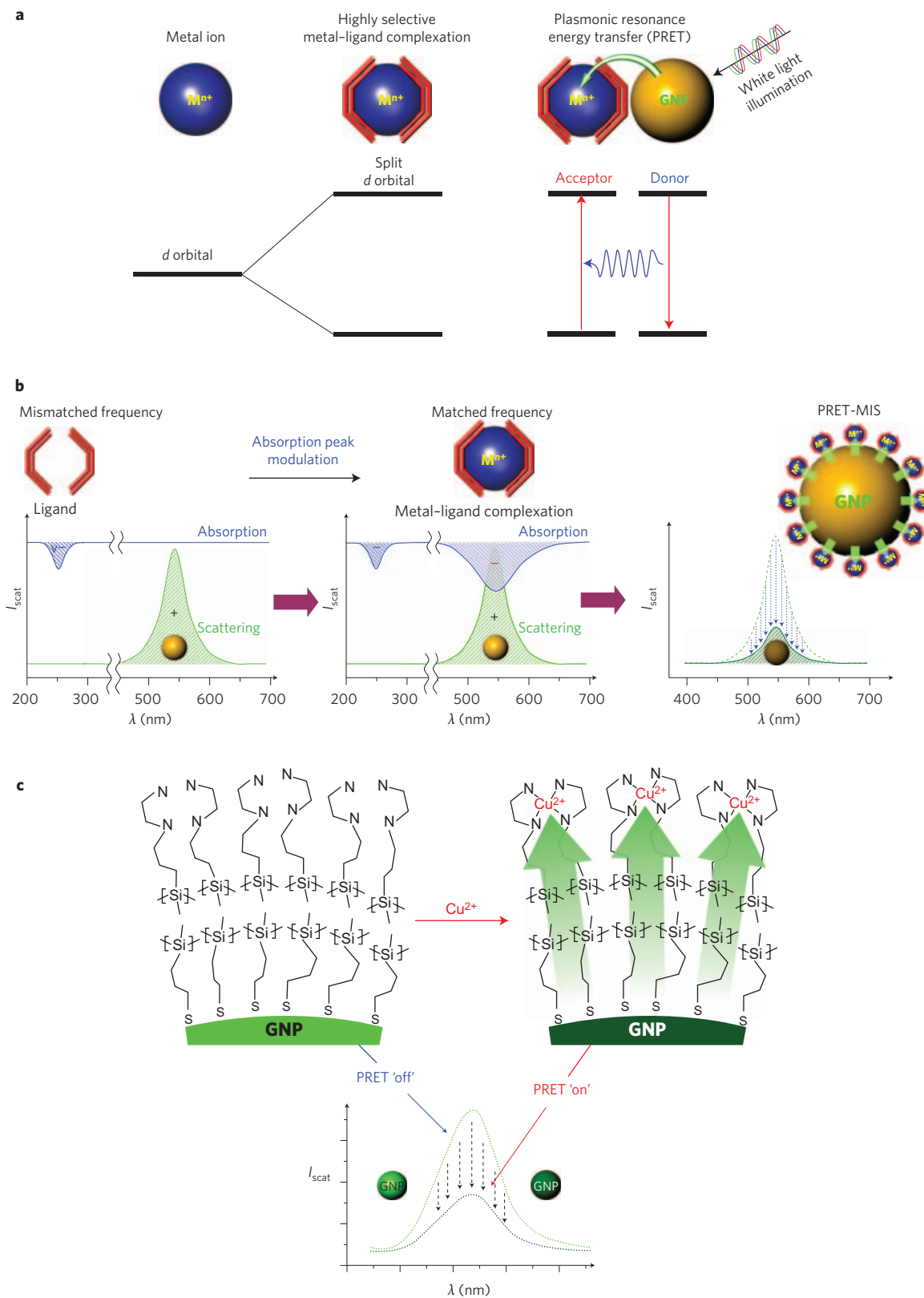


Figure 1 | Plasmonic resonance energy transfer-based metal ion sensing (PRET-MIS). **a**, When the transition metal ion (blue) binds with the matching ligand (red), *d* orbitals are split, which can generate a new absorption band of the metal-ligand complex in the visible range. Owing to the new absorption band, Rayleigh scattering energy from a gold nanoplasmonic probe (GNP) can be transferred to the metal-ligand complex. **b**, There is no spectral overlap between ligands without the metal ion and the GNP (left). When the electronic absorption frequency of the metal-ligand complex matches with the Rayleigh scattering frequency, the selective energy transfer is induced by this spectral overlap (middle) and the distinguishable resonant quenching on the resonant Rayleigh scattering spectrum is observed (right) **c**, A schematic illustrating the detection of Cu^{2+} via PRET between a single GNP and conjugated resonant complexes $[\text{Cu}(\text{TMSen})_2]^{2+}$ (the hydrogen atoms are not shown), and the expected Rayleigh scattering profile. I_{scat} , scattering intensity.

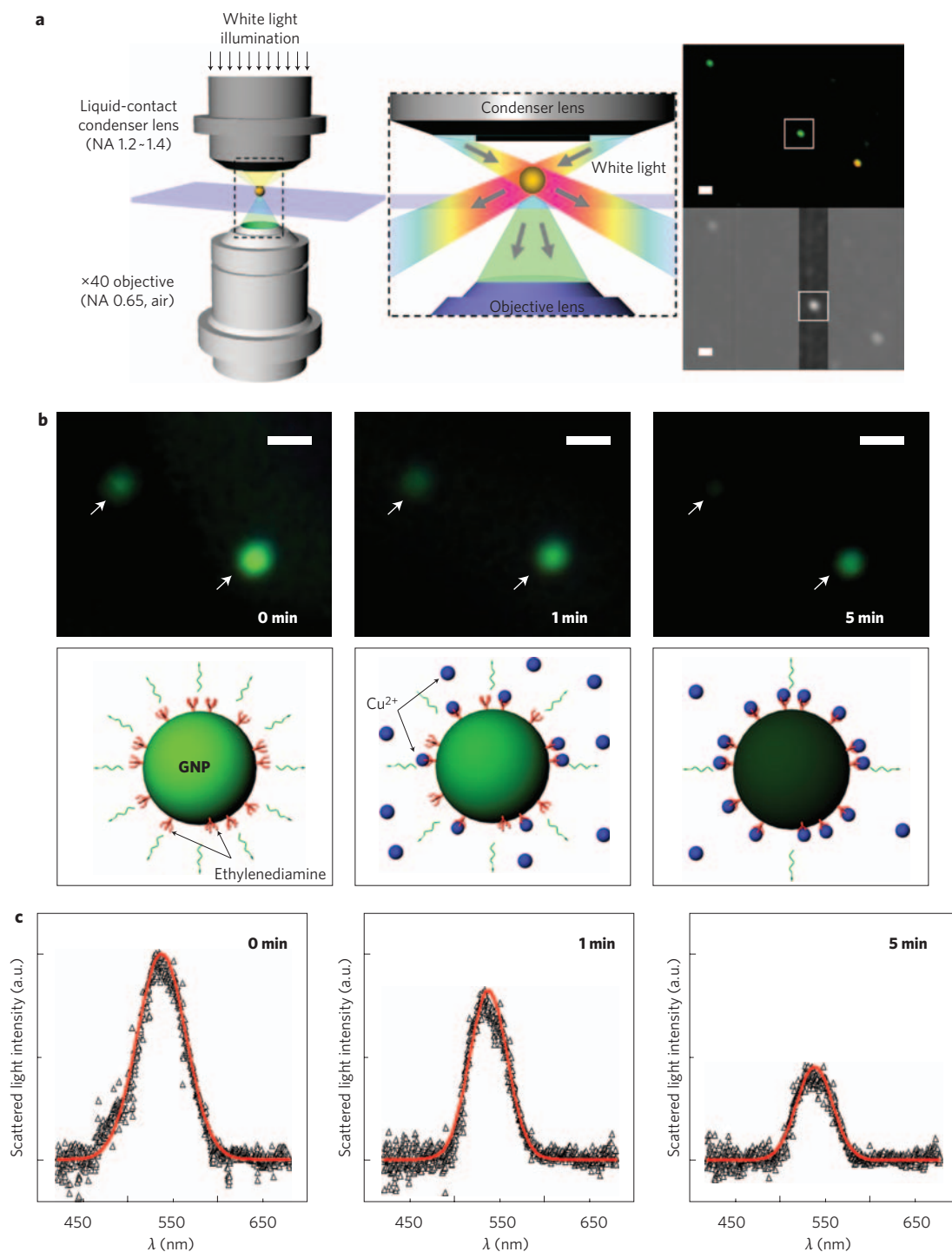


Figure 2 | Resonant quenching of a single gold nanoplasmonic probe by conjugated absorbing Cu²⁺ complexes. **a**, Detailed experimental configuration (left); enlarged schematic diagram of the oblique angle light excitation (middle); dark-field Rayleigh scattering image of GNPs on a colour CCD camera (top right), and corresponding zero-order spectrograph image (bottom right). A single GNP is targeted and isolated on the slides for spectroscopic examination. The scale bars represents 2 μm . NA, numerical aperture. **b**, Representative time-dependent true colour images (top) and corresponding schematics (bottom) of ethylenediamine (TMSen)-functionalized GNP after exposure with 10 mM Cu²⁺. The white arrow indicates a single GNP. The scale bars represents 2 μm . **c**, Corresponding Rayleigh scattering spectra of a single GNP. The black triangles represent the raw data; the red lines are Gaussian fitted curves.

probes were acquired using a dark-field microscopy system with a true-colour imaging charge-coupled device (CCD) camera and a spectrometer (Fig. 2a). Only a single probe showing the plasmon resonance peak centred at $\sim 530\text{--}540$ nm (typical FWHM bandwidth in our study is around 50 nm) with green colour was investigated. Aggregates, as judged by colour and scattering profile, were ruled

out in the following analyses. The total number of chelating ligands on a single gold nanoparticle was estimated to be $\sim 53,300$ (see Supplementary Information).

Coordination of Cu²⁺ with an ethylenediamine-functionalized probe leads to striking changes in the Rayleigh scattering profile. After five minutes of exposure to Cu²⁺, Rayleigh scattering exhibits

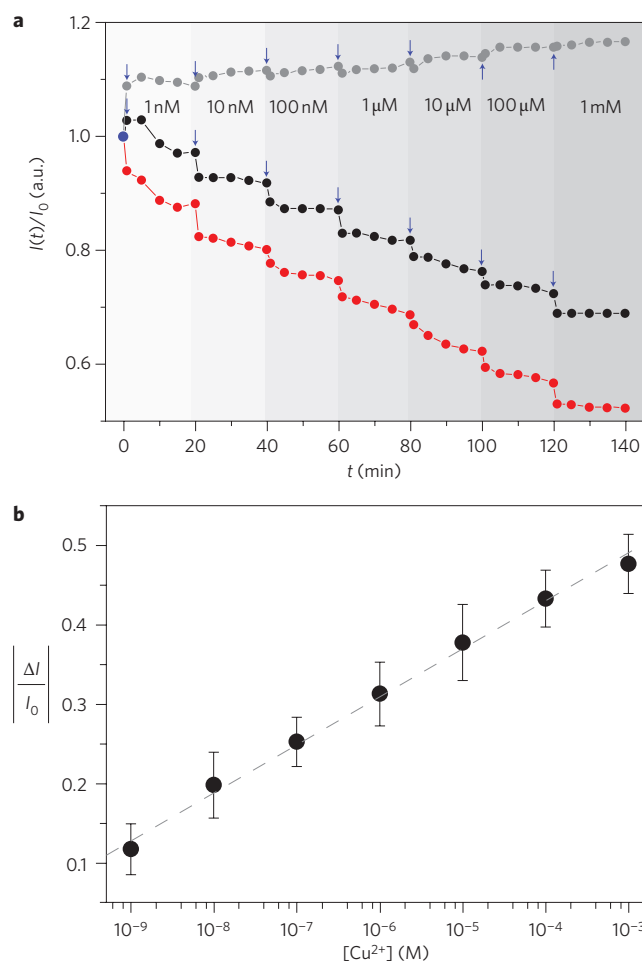


Figure 3 | Detection performance of the gold nanoplasmonic probe (GNP) system. a, Real-time detection of Cu^{2+} . Plot of normalized scattering intensity at the scattering maximum (λ_{max}), $I(t)/I_0$ versus time for a TMSen-modified GNP (black dots) and a control (without TMSen; grey dots) for concentrations ranging from 1 nM to 1 mM. The relative scattering intensity at each Cu^{2+} concentration for the unmodified GNP was subtracted from the relative scattering intensity for the TMSen-modified GNP to give the difference, providing a plot of the net change in the relative scattering intensity, $\Delta I(t)/I_0$ (red dots). The concentration values are indicated on the plot. Arrows mark the points when solutions were changed. The blue dot indicates the relative scattering intensity with deionized water. **b**, Equilibrium differential scattering intensity change, $|\Delta I/I_0|$ (taken as an absolute value for the sake of clarity) as a function of Cu^{2+} concentration. The dashed grey line is a logarithmic fitted to the Cu^{2+} concentration data points. Error bars are equal to ± 1 s.d. The regression coefficient (R^2) is 0.995.

a drastic decrease in intensity with a concomitant decrease in dark-field transmittance without any noticeable spectral shift ($\Delta\lambda_{\text{max}}$) (Fig. 2b,c). Such a significant spectral decrease without $\Delta\lambda_{\text{max}}$ cannot be explained by either a local refractive index change adjacent to the gold nanoparticles or direct optical absorption by the conjugated Cu^{2+} complexes. In fact, direct optical absorption by the conjugated complexes is several orders of magnitude too small to explain the current observations. The optical absorption only accounts for $<0.1\%$ of scattered light intensity loss even under the assumption of 100% excitation efficiency (not shown). Previous studies using single-particle plasmon resonance focused only on the shift of the resonant frequency due to the change of dielectric property of the particle's surroundings^{21,22}.

We attribute the current observations of the spectral decrease to resonant energy quenching of the gold nanoplasmonic probe by the

Cu^{2+} complexes. Previous studies of the surface plasmon-mediated FRET process^{23,24}, resonance peak shifts due to redox molecules²⁵ and surface plasmon quenching with quantum dots²⁶ imply the possibility of such energy transfer. Further evidence for the proposed PRET comes from previous experiments using cytochrome *c*¹¹. Interestingly, in the case of cytochrome *c* conjugation, the PRET process results in quantized quenching dips whose positions exactly correspond to the optical absorption peaks of cytochrome *c* (note that reduced cytochrome *c* has two peaks at 525 nm (FWHM of ~ 20 nm) and 550 nm (FWHM of ~ 12 nm)¹¹). Taken together, we concluded that the energy transfer from the gold nanoplasmonic probe to the metal–ligand complex could result in either a ‘spectral decrease’, as in this study, or in a quantized ‘spectral quenching dip’, depending on the broadness of the absorption band of the resonant molecules (see Supplementary Fig. S3)¹¹. We are currently exploring experimental and theoretical approaches to address the effect of the strength of the extinction coefficient, plasmon dependence, surface coverage and energy transfer distance dependence on PRET in greater detail.

Having established that the plasmon resonance energy could be transferred to surface Cu^{2+} complexes, we investigated the sensing performance of the probe in detail. To evaluate the sensitivity, different concentrations of Cu^{2+} from a single stock solution were tested. Figure 3a shows the normalized response of the particle to order-of-magnitude changes in Cu^{2+} concentration. The scattered light intensity of a single probe decreases rapidly (in ~ 5 min) to a constant value on addition of Cu^{2+} solution, and the normalized scattering intensity, $I(t)/I_0$, at λ_{max} shows a very similar systematic decrease with increasing Cu^{2+} concentration. By stark contrast, the control shows that addition of Cu^{2+} solution to gold nanoparticles lacking ethylenediamine ligands does not produce a change in scattered light intensity except an $8.8 \pm 3.5\%$ increase on the first exposure to Cu^{2+} solution. The regression coefficient in the equilibrium curve in Fig. 3b is higher than 0.99 (semi-log scale) for a concentration range from 1 nM to 1 mM. It is noteworthy that a single gold nanoplasmonic probe registers a substantial $11.0 \pm 3.1\%$ scattered light intensity decrease after 5 min of exposure to 1 nM Cu^{2+} . This response is significantly larger than the $<1.0\%$ drift in scattered light intensity of bare gold nanoparticles over 20 min. Our gold nanoplasmonic probe-based system is 100 to 1,000 times more sensitive than organic fluorophores, chromophore-based detection systems^{3–8} and even advanced gold nanoparticle-based systems¹⁰. Moreover, the metal ions can be dissociated from the complex, thus regenerating the probe, by simply washing with 1 M HCl for 1 h.

The selectivity of this system was explored by testing the response of the probe to other biologically and environmentally relevant metal ions, including Mg^{2+} , Ca^{2+} , Na^+ and K^+ at a concentration range of 100 nM to 100 μM . The bar graph in Fig. 4 summarizes the sensing response to other metal ions. With the exception of Cu^{2+} , treatments of other metal ions with free ethylenediamine ligands generate no colour change, nor are their respective absorbances in the UV-vis range (data not shown). As expected, upon exposure to other metal ions, our probe produces no discernible change in the scattered light intensity and $-\Delta I/I_0$ randomly fluctuates by 5% at most, irrespective of concentration, suggesting that only a resonant metal–ligand complex with an absorption profile similar to the scattering spectrum of a single probe could indeed be a receptor in the PRET process. Additional experiments with Co^{2+} and Ni^{2+} also confirm the selectivity for Cu^{2+} over other transition metal ions as the probe was ineffective despite these ions forming similar charge-transfer complexes with the chelating ligands used owing to the interaction of the *d*-orbital (Fig. 4). We attribute this remarkable selectivity to two key features of our detection system: exclusive complex formation only with the targeted metal ion, and energy transfer only in the case of a frequency-matching condition between the particle and the metal–ligand complex.

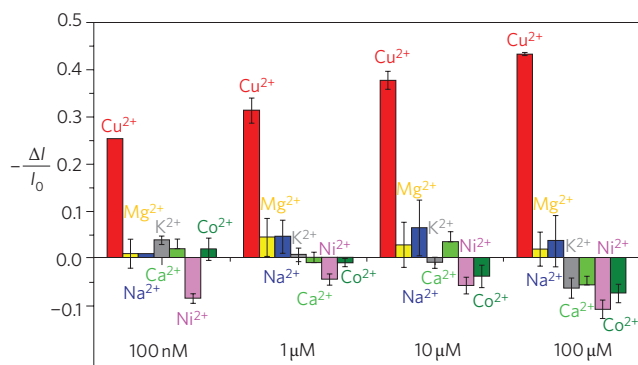


Figure 4 | Highly selective detection owing to selective Cu^{2+} complex formation and selective PRET. Bar graph summarizing the change in response of the functionalized gold nanoplasmonic probe to five environmentally and biologically relevant metal ions (Cu^{2+} , K^{+} , Ca^{2+} , Mg^{2+} , and Na^{+}) and two other transition metal ions (Co^{2+} and Ni^{2+}). The height of each bar, $-\Delta I/I_0$, represents the percent change in the scattered light intensity following 20 min of metal ion exposure. Error bars correspond to standard errors measured from 10 samples.

Briefly, we also applied PRET-based metal-ion sensing to detect the changes in intracellular Cu^{2+} in living HeLa cells, which are derived from cervical cancer. As expected, on exposure with 100 μM Cu^{2+} , the scattered light intensities collected from 30 different spots in a single cell (with TMSen-functionalized gold nanoparticles) represented a relative decrease of 31.2%, on average, compared with the control (with bare particles) (see Supplementary Figs S6–S8). More *in vivo* experimental characterizations are currently underway.

In conclusion, we have demonstrated that PRET-based metal-ion sensing can detect concentrations of Cu^{2+} down to 1 nM, and selectivity for Cu^{2+} over K^{+} , Na^{+} , Ca^{2+} , Mg^{2+} , Ni^{2+} , and Co^{2+} . This approach can also, in principle, be extended to detect other metal ions and various molecules by either substituting another resonant metal–ligand pair (or molecules) or by modulating the particle plasmon resonance positions (see Supplementary Fig. S4). The ability to resolve a single nanoparticle with a high sensing performance can be also used for the detection and visualization of metal ions in living systems.

Methods

Preparation of nanoplasmonic probe. Glass slides were cleaned in a piranha solution (30 min; warning: strong acidic oxidant, very harmful to personal contact). A cleaned glass slide was modified with 3-mercaptoptrimethoxysilane (MPTMS, Fluka) by incubation in 1 mM MPTMS isopropyl alcohol (IPA) for 24 h. The solution of MPTMS reacted with the surface to form a surface presenting thiol groups. The glass slide was then rinsed with acetone and IPA. 50-nm spherical gold particles were immobilized on the MPTMS-modified glass slide (24 h, under mild sonication). Freshly prepared particles on the glass slide were then immersed into 1 mM MPTMS for 24 h. For hydrolysis of the methoxy groups of MPTMS, the silane-functionalized particles were washed with ethanol and deionized water and immersed in a 0.1 M HCl solution for 1 h. Finally, the resulting gold plasmonic probes on the glass were immersed into 1 mM N-[3-(trimethoxysilyl)propyl]ethylenediamine (TMSen) solution for 24 h.

Scattering imaging and spectroscopy of a single nanoplasmonic probe. The microscopy system depicted in Fig. 2a consisted of a Carl Zeiss Axiovert 200 inverted microscope equipped with a dark-field condenser (NA 1.2 ~ 1.4), a true-colour digital camera (CoolSNAP cf, Roper Scientific) and monochromator (300 mm focal length and 300 grooves per mm, Acton Research) with a 1,024 × 256 pixel cooled spectrograph CCD camera (Roper Scientific). A 2- μm -wide aperture was placed in front of the monochromator to keep only a single probe in the region of interest.

Received 20 May 2009; accepted 31 July 2009;
published online 6 September 2009

References

- Lippard, S. J. & Berg, J. M. *Principle of Bioinorganic Chemistry* (University Science Books, 1994).
- Tsien, R. W. & Tsien, R. Y. Calcium channels, stores, and oscillations. *Annu. Rev. Cell Biol.* **6**, 715–760 (1990).
- Chang, C. J., Jaworski, J., Nolan, E. M., Sheng, M. & Lippard, S. J. A tautomeric zinc sensor for ratiometric fluorescence imaging: application to nitric oxide-induced release of intracellular zinc. *Proc. Natl Acad. Sci. USA* **101**, 1129–1134 (2004).
- Coronado, E. *et al.* Reversible colourimetric probes for mercury sensing. *J. Am. Chem. Soc.* **127**, 12351–12356 (2005).
- Ros-Lis, J. V., Marcos, M. D., Martinez-Manez, R., Rurack, K. & Soto, J. A regenerative chemodosimeter based on metal-induced dye formation for the highly selective and sensitive optical determination of Hg^{2+} ions. *Angew. Chem. Int. Ed.* **44**, 4405–4407 (2005).
- Zhu, X.-J., Fu, S.-T., Wong, W.-K., Guo, J.-P. & Wong, W.-Y. A near-infrared-fluorescent chemodosimeter for mercuric ion based on an expanded porphyrin. *Angew. Chem. Int. Ed.* **45**, 3150–3154 (2006).
- Mancin, F., Rampazzo, E., Tecilla, P. & Tonellato, U. Self-assembled fluorescent chemosensors. *Chem. Eur. J.* **12**, 1844–1854 (2006).
- Krämer, R. Fluorescent chemosensors for Cu^{2+} ions: fast, selective, and highly sensitive. *Angew. Chem. Int. Ed.* **37**, 772–773 (1998).
- Kim, Y., Johnson, R. C. & Hupp, J. T. Gold nanoparticle-based sensing of “spectroscopically silent” heavy metal ions. *Nano Lett.* **1**, 165–167 (2001).
- Lee, J.-S., Han, M. S. & Mirkin, C. A. Colourimetric detection of mercuric ion (Hg^{2+}) in aqueous media using DNA-functionalized gold nanoparticles. *Angew. Chem. Int. Ed.* **46**, 4093–4096 (2007).
- Liu, G. L., Long, Y., Choi, Y., Kang, T. & Lee, L. P. Nanoscopic biomolecular absorption spectroscopy enabled by single nanoparticle plasmon resonance energy transfer. *Nature Methods* **4**, 1015–1017 (2007).
- Gaggelli, E., Kozłowski, H., Valensin, D. & Valensin, G. Copper homeostasis and neurodegenerative disorders (Alzheimer’s, Prion, and Parkinson’s diseases and amyotrophic lateral sclerosis). *Chem. Rev.* **106**, 1995–2004 (2006).
- Jun, S. & Saxena, S. The aggregated state of amyloid- β peptide *in vitro* depends on Cu^{2+} ion concentration. *Angew. Chem. Int. Ed.* **47**, 3959–3961 (2007).
- Huang, X. *et al.* Cu(II) potentiation of Alzheimer A β neurotoxicity. *J. Biol. Chem.* **274**, 37111–37116 (1999).
- Brown, D. R. *et al.* The cellular prion protein binds copper *in vivo*. *Nature* **390**, 684–687 (1997).
- Que, E. L. & Chang, C. J. A smart magnetic resonance contrast agent for selective copper sensing. *J. Am. Chem. Soc.* **128**, 15942–15943 (2006).
- Zheng, Y. *et al.* Development of fluorescent film sensors for the detection of divalent copper. *J. Am. Chem. Soc.* **125**, 2680–2686 (2003).
- Klein, G., Kaufmann, D., Schürch, S. & Reymond, J.-L. A fluorescent metal sensor based on macrocyclic chelation. *Chem. Commun.* 561–562 (2001).
- Smith, R. M. & Martell, A. E. *Critical Stability Constants* (Plenum, 1975).
- Childs, W. R. & Nuzzo, R. G. Large-area patterning of coinage-metal thin films using decal transfer lithography. *Langmuir* **21**, 195–202 (2005).
- Liu, G. L. *et al.* Molecular ruler for measuring nuclease activity and DNA footprinting. *Nature Nanotech.* **1**, 47–52 (2006).
- Rascheke, G. *et al.* Biomolecular recognition based on single gold nanoparticle light scattering. *Nano Lett.* **3**, 935–938 (2003).
- Andrew, P. & Barnes, W. L. Energy transfer across a metal film mediated by surface plasmon polaritons. *Science* **306**, 1002–1005 (2004).
- Van Duyne, R. P. Molecular plasmonics. *Science* **306**, 985–986 (2004).
- Zhao, J. *et al.* Resonance surface plasmon spectroscopy: low molecular weight substrate binding to cytochrome P450. *J. Am. Chem. Soc.* **128**, 11004–11005 (2006).
- Romero, M. J., Lagemaat, J. v. d., Mora-Sero, I., Rumbles, G. & Al-Jassim, M. M. Imaging of resonant quenching of surface plasmons by quantum dots. *Nano Lett.* **6**, 2833–2837 (2006).

Acknowledgements

This work was supported by a grant from the Center for Nanostructured Materials and Technology under the 21st Century Frontier R&D Programs of the Korea Ministry of Science and Technology.

Author contributions

L.P.L. designed the nanospectroscopy research; Y.C. and T.K. conceived, designed and performed the experiments on selective ion detection; Y.P. fabricated functionalized gold nanoparticles for internalization into HeLa cells; Y.C., T.K. and L.P.L. wrote the paper.

Additional information

Supplementary information accompanies this paper at www.nature.com/naturenanotechnology. Reprints and permission information is available online at <http://ngp.nature.com/reprintsandpermissions/>. Correspondence and requests for materials should be addressed to T.K. and L.P.L.